Erschienen in: Journal of the American Chemical Society ; 133 (2011), 29. - S. 11154-11162
https://doi.org/10.1021/ja2010048

Transient Enzyme−Substrate Recognition Monitored by Real-Time NMR

Caroline Haupt,[†] Rica Patzschke,[†] Ulrich Weininger,[†,‡,#] Stefan Gröger,[†] Michael Kovermann,[†] and Jochen Balbach*[,†,‡]

[†]Institut für Physik, Biophysik and [‡]Mitteldeutsches Zentrum für Struktur und Dynamik der Proteine (MZP), Martin Luther Universität Halle Wittenberg, D 06120 Halle (Saale), Germany

ABSTRACT: Slow protein folding processes during which kinetic folding intermediates occur for an extended time can lead to aggregation and dysfunction in living cells. Therefore, protein folding helpers have evolved, which prevent proteins from aggregation and/or speed up folding processes. In this study, we present the structural characterization of a long living transient folding intermediate of RNase T1 (S54G/P55N) by time resolved NMR spectroscopy. NMR resonances of this kinetic folding intermediate could be assigned mainly by a real time 3D BEST HNCA. These assignments were the basis to investigate the interaction sites between the protein folding helper enzyme SlyD(1 165) (SlyD*) from *Escherichia coli* (*E. coli*) and this kinetic intermediate at a residue resolution. Thus, we investigated the Michaelis−Menten complex of this enzyme reaction, because the NMR data acquisition was performed during the actual catalysis. The interaction surface of the transient folding intermediate is restricted to a region around the peptidyl−prolyl bond (Y38−P39), whose isomerization is catalyzed by SlyD*. The interaction surface regarding SlyD* extends from specific amino acids of the FKBP domain forming the peptidyl prolyl *cis/trans* isomerase active site to almost the entire IF domain. This illustrates an effective interplay between the two functional domains of SlyD* to facilitate protein folding catalysis.

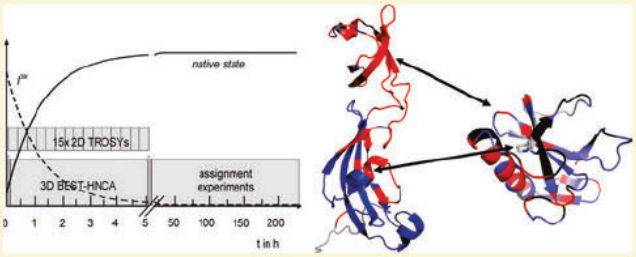

INTRODUCTION

Understanding assisted protein folding in detail is very important because an increasing number of diseases emerge that can be traced back to misfolded or aggregated protein chains.[1] During the last years, the improvement of experimental techniques opened the door for a more detailed understanding of the complex nature of protein folding. The combination of different methods such as circular dichroism (CD) and fluorescence spectroscopy,[2,3] FRET based single molecule spectroscopy,[4] real time NMR spectroscopy,[5,6] and NMR relaxation studies[6,7] with computer based simulations of molecular dynamics to analyze protein folding landscapes reveal a more comprehensive view of the protein folding process.[8] Small single domain proteins usually fold very fast to their native structure,[9−13] whereas larger proteins often pass through a harsh funnel shaped energy landscape to adopt the low energy native state.[14−16] The surface of such an energy landscape can lead to metastable, non native interactions during the folding process, which favors the formation of partially folded intermediates that in turn can decelerate the overall folding process or promote the formation of aggregated protein structures.[14−16] Although the basic knowledge about protein folding is quite broad, the question how cells cope with physiological relevant long living intermediate states is still under investigation.

Protein folding helper enzymes, or chaperones, were classified to handle those protein states by binding to hydrophobic patches of unfolded or partially folded polypeptide chains and thus prevent potential aggregation.[17−19] Besides the ubiquitous occurring chaperones, there exist several classes of folding catalysts that specifically accelerate potential slow steps in the protein folding process and therefore further lower the risk of aggregation. The most prominent examples are protein disulfide isomerases and peptidyl prolyl *cis/trans* isomerases (PPIases).[20,21] Some PPIases combine both chaperone properties and PPIase activity separated into different domains but acting synergetically, which leads to very efficient protein folding helper enzymes (e.g., SurA,[22] FkpA,[23−25] trigger factor,[26−28] and MtFKBP17[29]). The well characterized PPIase of the FK506 binding protein (FKBP) type SlyD(1 165) (SlyD*) from *Escherichia coli* (*E. coli*) is one of the folding helper enzymes harboring this dual behavior.[30−37] SlyD ("*sensitive to lysis*")[31] was initially discovered as a persistent contaminant of recombinantly purified proteins via immobilized metal ion affinity chromatography named WHP ("*wonderous histidine rich protein*")[30] suggesting one putative cellular function as a metallochaperone[38] that is involved in the

biosynthesis of hydrogenase 3 from *E. coli*.[39−41] Furthermore, during the Tat (*twin arginine translocation*) dependent translocation of folded proteins, SlyD binds and protects the unstructured signal peptides from proteolytic attack in the cytosol during the transport to the membrane,[35,42] which implies its chaperone properties as another putative physiological role. This physiological role as a chaperone was also supported by the fact that it stabilizes the hydrophobic protein E prior to insertion into the cell membrane during protein E mediated cell lysis by the phage ΦX174, giving the enzyme its name.[31]

Here, we investigated the catalysis of the isomerization of a peptidyl−prolyl bond by SlyD* on a highly resolved structural basis using the model substrate RNase T1 (S54G/P55N). RNase T1 is a small, 104 amino acids long, one domain protein whose folding mechanism has been well characterized during the last decades.[43−46] The protein contains four proline residues, two of them are in cis conformation in the native state (proline 39 and 55) and mainly determining the folding mechanism. The introduction of the *trans* peptidyl bond glycine 54/asparagine 55 (comparing the sequence of the homologue RNase C2[47]) simplifies the overall folding mechanism[43] and creates a variant (RNase T1 (S54G/P55N)) that shows only one slow refolding phase based on a long living native like intermediate I^{39t} with proline 39 in trans conformation: $U \rightarrow I^{39t} \rightarrow N^{39c}$. This variant is the standard substrate to quantify PPIase activity[48] and its folding intermediate was structurally characterized by NMR experiments.[5,49]

The present work focuses on the structural features of the interactions between the PPIase SlyD* and the long living kinetic folding intermediate of RNase T1 (S54G/P55N). The method of choice to gain structural and kinetic information at molecular resolution along the entire protein chain during the catalyzed refolding process is real time NMR spectroscopy. First, directly detected kinetic processes were performed by recording short consecutive one dimensional (1D) proton spectra using a rapid mixing device inside the NMR probehead for analyzing the folding of α lactalbumin,[50,51] RNase T1 (S54G/P55N),[5] lysozyme,[52,53] and barstar.[54,55] But the applicability is limited to only a few resonances because of the crowded, highly overlapped nature of 1D ^{1}H NMR spectra. These problems can be avoided by multidimensional experiments. Unfortunately, the time resolution gets low due to the time expense required to correlate additional frequencies. Hence, the application of multidimensional real time NMR experiments was restricted to very slow protein folding reactions. Thus, a faster indirect strategy was introduced in which the kinetic information is encoded in the line shape of the respective resonances of a two dimensional (2D) spectrum recorded during the whole refolding time.[5,56]

In the past years, the progress in NMR spectroscopy led to the development of fast multidimensional acquisition methods with constant high spectral quality and sensitivity.[57] Several aspects have been addressed like minimizing the data points for the indirect dimensions (GFT spectroscopy,[58,59] projection reconstruction;[60,61] HADAMARD NMR;[62,63] single scan NMR,[64] sparse sampling[65]) or reducing the recycle delay. The latter one is achieved by accelerating the regain of equilibrium magnetization using Ernst angle excitation[66,67] and/or applying band selective pulses which correspond to a minimal excitation of aliphatic and water protons and hence to a smaller spin−lattice relaxation time (2D *band selective optimized flip angle short transient* SOFAST HMQC; 3D *band selective excitation short transient* BEST experiments).[68−73] Now, molecular kinetic processes on a second or minute time scale can be explored by 2D[74] and 3D correlation experiments on a time resolved level giving spectacular insights into molecular processes and therefore the opportunity to enlighten elementary steps in the overall protein folding process.

In the present paper, we describe to our knowledge the first structural characterization of a transient protein folding intermediate bound to a protein folding helper enzyme during catalysis. The backbone assignment of the transient folding intermediate was achieved using the fast pulsing BEST HNCA NMR method in the absence and presence of SlyD*. We could clearly restrict the interaction sites with SlyD* in the folding intermediate of RNase T1 (S54G/P55N) to the region where the isomerizing peptidyl−prolyl bond is located. For the folding helper enzyme SlyD*, a dynamic interplay between its two functional domains the chaperone domain and the FKBP domain has been observed.

MATERIALS AND METHODS

Materials and Reagents. Guanidiniumhydrochloride ultrapure was purchased from MP Biomedicals (Solon, OH). All other chemicals were of analytical grade and from VWR (Darmstadt, Germany), Roth (Karlsruhe, Germany), or Sigma Aldrich (St. Louis, MO).

Gene Construction, Protein Expression, and Purification. RNase T1 (S54G/P55N) and SlyD* (*E. coli* SlyD(1 165)) were expressed and purified as previously described.[75−77] ^{15}N and ^{13}C labeling was performed using M9 minimal medium containing 1 g/L ^{15}N NH_4Cl and 4 g/L ^{13}C glucose for expression; unlabeled protein was expressed in dYT medium.

NMR Measurements. All NMR spectra were acquired with a Bruker Avance III 600 MHz or 800 MHz spectrometer in 10 mM Bis Tris (pH 6.0), containing 10% (v/v) D_2O, at 10 °C (monitoring isotope labeled RNase T1 (S54G/P55N)) or in 10 mM Tris (pH 7.5), containing 10% (v/v) D_2O, at 20 °C (monitoring isotope labeled SlyD*). The 800 MHz spectrometer was equipped with a cryogenic triple resonance probe. To monitor the refolding kinetics of RNase T1 (S54G/P55N), a series of 2D ^{1}H/^{15}N TROSY HSQC spectra was recorded with a time resolution of 20 min. For the ^{15}N SlyD* monitored refolding reaction, 2D ^{1}H/^{15}N TROSY HSQC spectra were recorded at intervals of 10 min. To get the backbone assignment of the intermediate state, a 3D BEST HNCA[68,73] was recorded using 64 and 96 increments in the ^{15}N and ^{13}C dimension, respectively. The interscan delay time was set to 200 ms; the offset for the band selective pulse was 8.4 ppm with a band width of 4 ppm. The overall acquisition time was 5 h. For backbone assignment of the native state of RNase T1 (S54G/P55N), HNCA, HNCACB, HN(CO)CACB, ^{15}N edited ^{1}H/^{15}N NOESY HSQC, and ^{1}H/^{15}N TOCSY HSQC were measured after the refolding was completed (Scheme 1). All NMR spectra were processed using NMRPipe[78] and analyzed using NMRView.[79]

The narrow white bars marked with an asterisk symbolize in scheme1 a short 2D ^{1}H/^{15}N TROSY HSQC spectrum recorded before and after the 3D BEST HNCA (recording time 5 min). The subsequent assignment experiments included 3D HNCA, HNCACB, HN(CO)CACB, and ^{15}N edited NOESY and TOCSY. During a second experiment, 15 2D ^{1}H/^{15}N TROSY HSQC spectra were sequentially recorded.

Refolding Experiments. ^{15}N RNase T1 (S54G/P55N) was unfolded in 6 M GdmCl, 10 mM Bis Tris (pH 6.0) overnight. Refolding was initiated by 10 fold dilution into refolding buffer (10 mM Bis Tris (pH 6.0), containing 10% (v/v) D_2O) giving a final protein concentration of 875 μM. For the catalyzed refolding reaction, 87.5 μM SlyD* (10% relative to RNase T1 (S54G/P55N) concentration) was provided in the refolding buffer. Experimental dead time was about 3−5 min until

Scheme 1. Illustration of the Experimental Workflow of the NMR Spectra Acquisition during Refolding of Isotope Labeled RNase T1 (S54G/P55N) Represented by a Dashed Line for the I^{39t} and a Solid Line for the Native State

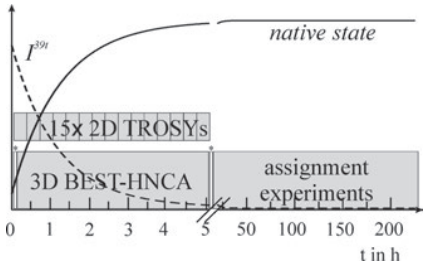

data acquisition started. Analogous conditions were used for recording the BEST HNCA during the refolding of $^{13}C/^{15}N$ RNase T1 (S54G/P55N) in the absence and in the presence of SlyD*. All these experiments were performed at 10 °C. To maintain high spectral quality for the ^{15}N SlyD* monitored refolding, 10 mM Tris (pH 7.5) was used as refolding buffer. This experiment was performed at 20 °C and at a higher concentration of ^{15}N SlyD* (400 μM, 33% relative to RNase T1 (S54G/P55N) concentration, 1.2 mM). Moreover, the final concentration of 0.6 M GdmCl was quickly removed via a PD10 column directly after starting the refolding reaction. The buffer exchange was performed at 4 °C to keep refolding as slow as possible. A spectrum of free SlyD* was recorded under analogous conditions as a control experiment.

RESULTS

Assignment of the Transient Folding Intermediate of RNase T1 (S54G/P55N). In NMR spectra, recorded during protein folding reactions retarded by highly populated intermediates, resonances of both the intermediate(s) and the native state occur and can be analyzed at a residue by residue resolution. Typically, the kinetics of the folding reaction can be easily followed based on the resonances of the native state (N), because those can be assigned under native equilibrium conditions.[5,80] The additional resonances in the kinetic NMR spectra must result from the intermediate state(s) (I). Here, unambiguous assignments are much more difficult to obtain.

Conventional 3D NMR backbone assignment experiments, which correlate the NMR active nuclei ^{1}H, ^{13}C, and ^{15}N typically take 1 to 2 days of measurement time. From fluorescence and 1D ^{1}H NMR spectroscopy monitored refolding kinetics of RNase T1 (S54G/P55N), it is known that the lifetime of the transient folding intermediate is only about 5 h under the given experimental conditions (Supporting Information Figure S1). Using the BEST approach[68,73] for measuring 3D correlation spectra, it is possible to record an HNCA experiment with reasonable signal to noise and spectral resolution within one or few hours.

For the assignment of the NMR resonances of the transient folding intermediate I^{39t} of RNase T1 (S54G/P55N), we recorded one 3D BEST HNCA during the 5 h refolding time (see scheme 1 in the Material and Methods section) using an interscan delay time of 200 ms compared to 1 s for a conventional HNCA experiment. This spectrum contains resonances of both I^{39t} and the native state N. For complete assignments of N under these conditions, we recorded directly after the refolding had finished conventional 3D HNCA, HNCACB, HN(CO)CACB, and ^{15}N edited NOESY and TOCSY experiments. These assignments

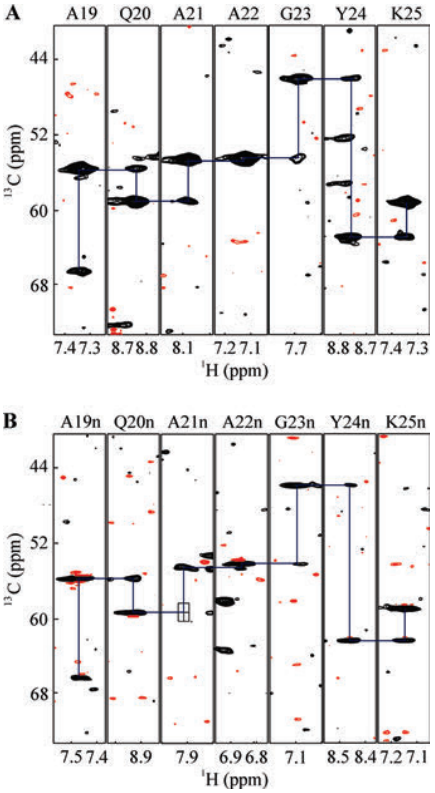

Figure 1. $^{1}H/^{13}C$ strips from a selected sequence range of the 3D BEST HNCA recorded during the catalyzed refolding of RNase T1 (S54G/P55N) at pH 6.0 and 10 °C. Connectivities in the region of C^{α} resonances of A19−K25 of the (A) intermediate I^{39t} and (B) the native state N are indicated by solid lines (black, positive signal intensities; red, negative signal intensities). The sequential cross peak of A21n (indicated by the reticule) is not visible at this contour level.

were used to identify all resonances originating from the native state in the 3D BEST HNCA. All additional resonances belong to I^{39t}, which could subsequently be sequentially assigned. Further help came from the two 2D $^{1}H/^{15}N$ TROSY HSQC spectra recorded before and after the 3D BEST HNCA. The first contains resonances of both I^{39t} and N, whereas the later one contains only resonances of N. Therefore, the ^{1}H and ^{15}N chemical shifts of each cross peak in the 3D BEST HNCA could be assigned either to the I^{39t} or the N state. This assignment was verified by inspection of the series of 15 2D $^{1}H/^{15}N$ TROSY HSQC spectra recorded during a second refolding experiment (see below). All further assignments were performed by a conventional HNCA analysis approach, which also solved signal overlaps between ^{1}H and ^{15}N correlations of I^{39t} and N in the 2D $^{1}H/^{15}N$ TROSY HSQC spectra (e.g. Q20(I^{39t}) and F100(N) both resonate at 118.5 ppm (^{15}N) and 8.68 ppm (^{1}H)).

Sixty three residues out of 104 clearly show in I^{39t} distinct chemical shifts compared to the native state and could be assigned. One sequential walk from A19 to K25 is shown in Figure 1. Sixteen further amino acids of I^{39t} have identical chemical shifts compared to the native state. These amino acids symbolize the regions in the intermediate state that are already in a native like environment. Altogether, the backbone of 78% of all residues could be assigned for the folding intermediate I^{39t} and 98% for the native state (Figure 2, Figure S3). No additional cross

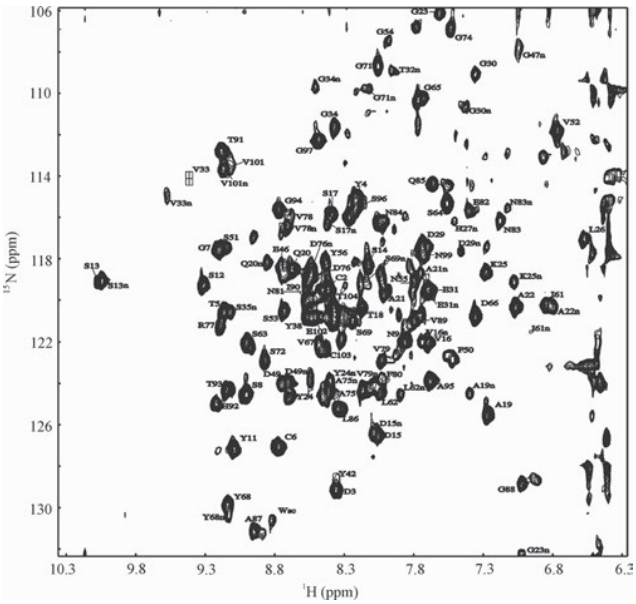

Figure 2. Backbone assignment of the cross peaks of RNase T1 (S54G/P55N) in 10 mM Bis Tris, pH 6.0, 0.6 M GdmCl, and 10 °C for the kinetic folding intermediate recorded during the first 20 min of refolding (see Scheme 1). The assignment is given for the intermediate; already existent cross peaks for the native state are marked with n. The resonance of V33 of I^{39t} is not visible at the depicted contour level. Distortions at 6.5 ppm arise from the 0.6 M GdmCl.

peaks for the missing amino acids, which are mainly located in the loop region around proline 39, could be found in the spectra.

During the 3D BEST HNCA, the ^{13}C dimension was incre mented along the real refolding time (see Scheme 1 in the Material and Methods section). Therefore, the line shape along this frequency axis should be affected, because the population of I^{39t} decreases and the population of N increases.[5,56] This results in broader lines for I^{39t} (Figure 1A) and a sharp central line accompanied by two broader negative contributions for N (see, e.g., A19 in Figure 1B, and line shape simulations in Figure S4).

The structural properties of the transient folding intermediate mapped onto the structure of RNase T1 illustrate the amino acids that are not yet native like (Figure 3D). They mainly comprise most of the α helix, the central β sheet, and the loop regions connecting these elements (Figure S6). β Strands stabilized by disulfide bonds are already at their native position in the inter mediate state. These results confirm previous findings, where H/D exchange experiments and the analysis of NOE distances in the intermediate state have shown that the secondary structure of the α helix is already formed but not yet in its native position.[5] The assignments of the backbone resonances of the intermediate state allowed to determine its secondary structure by the chemical shift index based on the C_α resonances[81] (Figure S2B). The majority of the secondary chemical shifts coincide between I and N. The main differences are located at the C terminal half of the α helix and the following loop, which also comprises Pro39. This finding coincides with analysis of the ^{1}H−^{15}N chemical shifts. Additionally, this region gets mainly recognized by the peptidyl prolyl *cis/trans* isomerases SlyD* (see below).

Monitoring the Catalysis of Proline-Limited Refolding by 2D NMR Spectroscopy in View of the Substrate RNase T1 (S54G/P55N). Knowing the backbone assignment of the kinetic folding intermediate (I^{39t}) and the native state (N) (Figure S3) allowed us to follow the refolding kinetics of RNase T1 (S54G/P55N) on both states (N and I^{39t}) in real time by a series of 2D ^{1}H/^{15}N TROSY HSQC spectra in the absence and presence of the PPIase SlyD*. The respective first spectra represent the spectrum for the intermediate state (Figure 3A,B; full spectrum in Figure S5). The high dispersion in the spectra confirms the high amount of tertiary structure and the already native like conformation of the intermediate state.[5,82] Analyzing the kinetics in detail by fitting a single exponential function to the peak volume of each cross peak provides time constants for refolding of 170 min for the uncatalyzed and 83 min for the catalyzed reaction, which is, as expected (Figure S1A,B1), 2 times faster (Figure 3C). The difference in signal intensity for the catalyzed and uncatalyzed refolding reaction is due to a lower protein concentration caused by slight aggregation as the uncatalyzed refolding was started by dilution of the highly concentrated unfolded RNase T1 (S54G/P55N). The missing aggregation behavior during the catalyzed refolding directly demonstrates the positive influence of the chaperone domain in SlyD*.

Binding Site for SlyD* in the Transient Folding Intermediate of RNase T1 (S54G/P55N). A comparison of the NMR spectra of the intermediate state from the uncatalyzed and catalyzed reaction reveals the interaction sites of the PPIase SlyD* with I^{39t} during refolding (Figure 4B,C; complete spec trum Figure S7). Most of the cross peaks show the same chemical shifts in the free and in the bound form indicating that most of the amino acids of the kinetic intermediate are not involved in an interaction with SlyD* (Figure S8). Cross peaks for residue tyrosine 24 for example show different chemical shifts between free and bound form (Figure 4B). An overview of the amino acids which represent the interaction site of SlyD* with I^{39t} are depicted in Figure 4C. It is clearly shown that SlyD* does not interact with that part of the intermediate which has already adopted the native structure. Moreover, SlyD* shows very specific interaction with the region where proline 39 is located, namely, the loop regions around the peptidyl−prolyl bond between tyrosine 38 and proline 39 and the C terminal part of the α helix in close proximity to the prolyl bond to be isomerized. This is also the main region, which deviates in the secondary chemical shifts between the I and the N state (Figure S2B).

Monitoring the Catalysis of Proline-Limited Refolding by 2D NMR Spectroscopy of the PPIase SlyD*. The data shown so far enlightened the structural effects on the substrate (^{15}N RNase T1 (S54G/P55N)) during the SlyD* mediated catalysis. To complete the picture of the interaction sites between the PPIase and the transient substrate, the refolding experiment was re peated using ^{15}N SlyD* and unlabeled substrate. To get a good signal to noise ratio, the experimental conditions were slightly changed. Instead of taking 10% SlyD* compared to the RNase T1 (S54G/P55N) concentration, 33% SlyD* was applied and GdmCl was removed directly after starting the refolding reaction prior the measurement. Because of the faster refolding under these conditions, ^{1}H/^{15}N TROSY HSQC spectra were taken every 10 min. The overlay of the ^{15}N SlyD* spectrum without RNase T1 (S54G/P55N) and the first spectrum recorded during refolding reveals many cross peaks that disappear upon complex formation during the catalysis indicating an extensive interaction between enzyme and substrate (Figure 4A, complete spectrum Figure S9). Thereby, amino acids from the FKBP domain as well as from the IF domain are involved (Figure 4A,C). Whereas almost the complete IF domain is involved, only residues of the

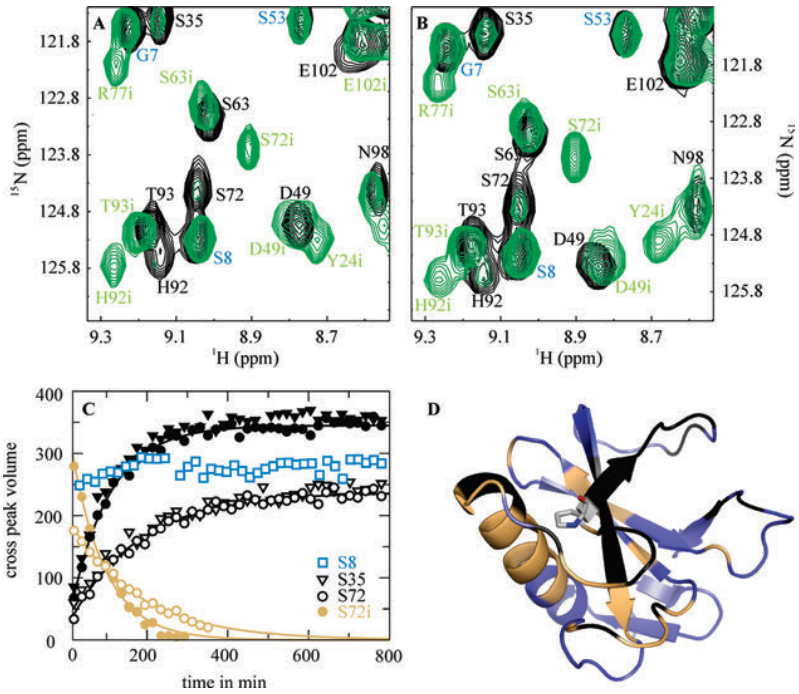

Figure 3. 2D NMR monitored refolding kinetics of RNase T1 (S54G/P55N) at pH 6.0 and 10 °C. (A and B) Section of $^{1}H/^{15}N$ TROSY HSQC spectra of 875 μM RNase T1 (S54G/P55N) at the beginning (green, intermediate state) and at the end (black, native state) of refolding in the absence (A) and presence of 87.5 μM SlyD* (B). The respective assignment is indicated. (C) Refolding kinetics derived from the increase and decrease in the absolute peak volume for residues S35 and S72 (black, native state; gold, intermediate state; blue, already native like in the intermediate state). Open symbols represent the uncatalyzed refolding, closed symbols the catalyzed refolding. Fitting a single exponential function to the data provides the following refolding rates: 0.306 ± 0.024 h^{-1} (S35), 0.612 ± 0.024 h^{-1} (S35, catalyzed), 0.354 ± 0.018 h^{-1} (S72), 0.780 ± 0.024 h^{-1} (S72, catalyzed), 0.354 ± 0.012 h^{-1} (S72, intermediate state), and 0.612 ± 0.036 h^{-1} (S72, intermediate state, catalyzed). Indicated errors result from the fitting procedure. (D) Model of RNase T1. Amino acids that are already in a native like environment (such as S8 also depicted in A, B, and C) in the intermediate state are colored blue. Amino acids of the latter group are indicated in blue in A and B. Amino acids whose respective cross peaks show different chemical shifts in the native and intermediate state and an increase in signal intensity during refolding are shown in gold. Proline 39 is depicted in stick representation. Unassigned residues are colored in black. Figure was created using PyMol (DeLano Scientific LLC, 2006).

PPIase active site in the FKBP domain are influenced during the catalysis.

DISCUSSION

The folding mechanism of the model substrate RNase T1 (S54G/P55N) has been investigated in the past in great detail.[43−46] The slow trans to cis isomerization of the petidyl prolyl bond between tyrosine 38 and proline 39 synchronizes the cooperative refolding of the long living kinetic folding intermediate (I^{39t}).[49] First, NMR measurements to characterize the transient folding intermediate were restricted to conventional NMR techniques and only allowed an incomplete view of the folding intermediate.[5,82] The main purpose of the present work was an extensive NMR characterization of I^{39t} and its interaction with the protein folding helper enzyme SlyD*, which comprises both peptidyl prolyl *cis/trans* isomerase and chaperone activities.

As a first step, the NMR assignment of the intermediate I^{39t} was required. To get a favorable time window for the NMR measurements with and without SlyD* catalysis, the experimental conditions were set to 10 °C and Bis Tris buffer at pH 6.0. Under these conditions, the lifetime of I^{39t} is 5 h, which was still not sufficient enough to record conventional 3D NMR experiments required for backbone assignment. However, by acquiring the fast pulsing 3D BEST HNCA in real time lasting 5 h, 78% of all NMR resonances of I^{39t} could be assigned. The structural properties of the kinetic folding intermediate consist of an already native like β sheet structure stabilized by two disulfide bonds. The only α helix has already formed, but not in its native position, confirming earlier 2D NOESY experiments.[5,49]

We then looked at the SlyD* mediated acceleration of the refolding of I^{39t}. The NMR assignment of the folding intermediate in the presence of SlyD* was also achieved by recording a 3D BEST HNCA under analogous conditions as for the uncatalyzed refolding of I^{39t}. The interaction sites of SlyD* with I^{39t} could be clearly localized (Figure 4): concerning the substrate RNase T1 (S54G/P55N), only the region around the peptide bond of proline 39, where the prolyl isomerization takes place, gets in close contact with SlyD*. Not yet native regions in I^{39t} remote from P39, such as the N terminal part of the α helix and the two β strands 76−81 and 86−91, do not get in direct contact with SlyD*. Note that all not yet native regions (gold in Figure 3D) change their conformation toward the native state as a consequence of the peptidyl−prolyl bond isomerization. Concerning the enzyme, the complete IF domain of SlyD* and all amino acids from the active site in the FKBP domain are involved in the interaction with the transient folding intermediate. For the archaeal SlyD homologue MtFKBP17, which also consists of the two functional domains (FKBP and IF domain) and which shows the same overall topology like SlyD*, a synergistic interaction between both domains during the catalyzed protein folding reaction was assumed.[29] This assumption could now be

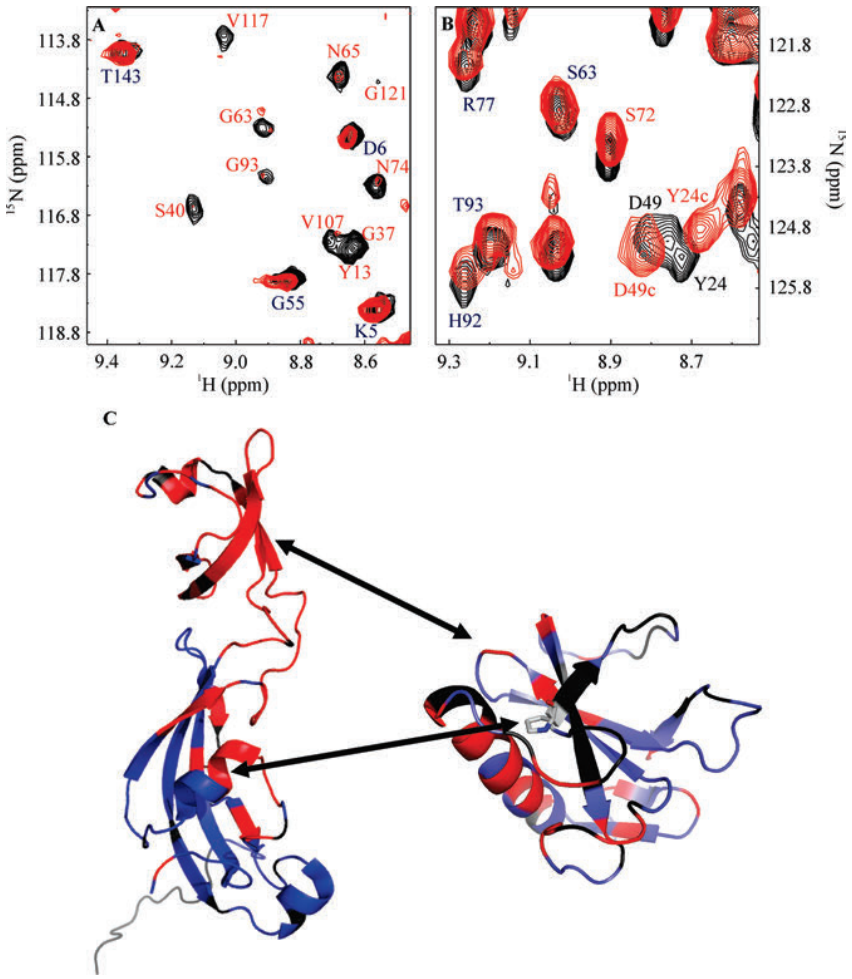

Figure 4. Binding interface between the transient protein folding intermediate I^{39t} and the protein folding helper enzyme SlyD* during the catalyzed refolding reaction of RNase T1 (S54G/P55N) at pH 6.0 and 10 °C. (A) Section of $^{1}H/^{15}N$ TROSY HSQC spectra of ^{15}N SlyD* in the free form (black) and in complex with the transient folding intermediate (red). The assignment of SlyD* is indicated for interacting amino acids (red, same color coding as in C) and noninteracting amino acids (blue). (B) Section of $^{1}H/^{15}N$ TROSY HSQC spectra of the intermediate state I^{39t} of ^{15}N RNase T1 (S54G/P55N) in the free, uncatalyzed form (black) and in complex with SlyD* (red). The assignment of I^{39t} is indicated for interacting amino acids (red, same color coding as in C) and noninteracting amino acids (blue). (C) Interacting amino acids of the kinetic folding intermediate (right) as well as of SlyD* (left) are mapped in red onto the respective structure. Those were derived from the chemical shift perturbation analysis between the uncatalyzed and catalyzed refolding reaction (A and B). Unchanged amino acids are shown in blue and indicate no interaction between the folding intermediate I^{39t} and the PPIase SlyD*. Unassigned amino acids and prolines are colored in black. Proline 39 of RNase T1 is depicted in stick representation. The lower arrow points toward the active PPIase site of SlyD* in the FKBP domain.

proven in real time on a molecular level for SlyD* from *E. coli* catalyzing the proline limited refolding of RNase T1 (S54G/P55N). Both domains are directly involved in the PPIase activity. This domain communication has also been observed during an equilibrium NMR titration experiment with the permanently unfolded substrate analogue RCM RNase T1 (S54G/P55N) (*reduced and carboxymethylated* RNase T1 (S54G/P55N)), where both domains showed substantial chemical shift changes upon binding,[35] but of course without substrate turnover. In summary, we could gain from the real time NMR experiments structural insights into the Michaelis−Menten complex between SlyD* and its protein substrate.

During the catalyzed refolding reaction, 10% of SlyD* relative to the substrate concentration was applied. Nevertheless, all of the I^{39t} molecules of the substrate show one defined set of chemical shifts in the SlyD* interacting form. This indicates fast exchange on the NMR time scale, which causes averaging of the I^{39t} molecules during the experience of SlyD* binding. Slow exchange on the NMR time scale would generate a separate set of resonances for 10% of the bound substrate molecules, which we do not observe. During the before men tioned equilibrium NMR titration experiments with RCM RNase T1 (S54G/P55N), the fast exchange limit was also monitored.[35] This is consistent with the classical Michae lis−Menten mechanism with a rapid association and dissocia tion of the enzyme−substrate complex compared to a low turnover number. For the standard PPIase activity assay using RCM RNase T1 (S54G/P55N)[48] and SlyD* at 15 °C and pH 7.5, the turnover number is indeed 0.5 s^{-1} and K_M, describing the pre equilibrium, is 0.38 μM.

The comparison of the NMR spectra after refolding has finished in the absence and presence of SlyD* led to a surprising

observation. Several residues showed chemical shift deviations between the free and bound state. Mapping these differences on the structure of RNase T1 revealed very similar residues com pared to the set of residues found to interact with SlyD* during catalysis (red residues in Figure S10, chemical shift perturbation analysis in Figure S11) including residues 4, 7, 13, 26, 29, 50, 55, 82, 103, and 104. Some differences comprise residues at the C terminus of the α helix and β strand 4. Note that this information comes from two pairs of cross peaks at different chemical shift positions, but all correspond to the same residue. For example, D49 shows $^{1}H/^{15}N$ chemical shifts in the inter mediate state of 8.80/124.7 ppm in the absence and 8.77/124.4 ppm in the presence of SlyD* (Figure 4), respectively, whereas in the native state, 8.73/124.2 ppm in the absence and 8.79/124.8 ppm in the presence of SlyD* (Figure S10). We assume that the final product after catalysis, which is the folded RNase T1 (S54G/P55N) with the peptide bond Y38−P39 in the *cis* conformation, still has some affinity to SlyD*, which can be resolved at the high NMR concentrations. Previous studies by NMR[5,49] showed native like properties of I^{39t} and even some remaining biological activity.[46] The latter observation was chal lenged by a recent study under conditions where the population of an enzyme−substrate or enzyme−product complex was negligible.[83] We assume here that I^{39t} and the native state are close enough in their structural properties so that SlyD* can form both an enzyme−substrate and enzyme−product complex, which can be characterized by NMR.

The kinetic NMR experiments revealed further the important role of the IF domain during PPIase activity. Previous results characterizing the chaperone activity of SlyD* showed that short hydrophobic peptides and permanently unfolded proteins such as RCM α lactalbumin or RCM RNase T1 (S54G/P55N) predominantly bind to the IF domain.[35] The isolated FKBP domain shows no chaperone activity. The isolated IF domain is unfolded but can be stabilized by ammonium sulfate and shows then chaperone activity (data to be published elsewhere). The isolated IF domain of a thermophilic homologue of SlyD is fully folded under high salt conditions with self contained chaperone activity.[38] We now extended our view of the IF domain by monitoring catalysis using real time NMR spectroscopy and showed that there exists a synergistic interplay between the IF domain and the catalytically active FKBP domain. This allows further conclusions for the mechanism of this protein folding helper enzyme. We assume that SlyD* picks up unfolded or partially folded elongated protein chains by its chaperone domain and directs them to the PPIase active site enhancing the local substrate concentration.

The importance of the IF domain is further accentuated by mutational analyses where the loop region of *human* FKBP12 (*h*FKBP12) was replaced by the IF domain of SlyD*.[84] The catalytic activity of this variant concerning prolyl isomerization in protein substrates was increased 200 fold compared to *h*FKBP12. The well established chaperone function of the IF domain in SlyD* recently found an application for *in vitro* diagnostics.[34,85] Several immunoassays derived from fusion con structs with SlyD* are already on the market. Taken together, SlyD* reveals many properties that can be adapted to protein engineering processes. Beyond that, implications for possible *in vivo* functions of SlyD were given. SlyD was identified to replace DnaK in the Tat dependent transport system as binding partner for hydrophobic signal peptides.[35,42] Its chaperone function is also exploited in the biosynthetic pathways of NiFe hydrogenases in *E. coli*[39,41] as well as of urease in *Helicobacter pylori*.[86,87] Heat shock experiments in *E. coli* showed an increase in the SlyD concentration compared to stress free conditions in the cell.[88] It was discovered that SlyD supports the folding of cytosolic proteins and keeps aggregation prone proteins in solution after the heat shock treatment. Altogether, SlyD is a multifunctional ubiquitous protein folding helper enzyme.

CONCLUSION

The application of multidimensional real time NMR spectro scopic techniques to study slow protein folding reactions has been established in the present work. They allowed the assignment of NMR resonances of a transient protein folding intermediate. On the basis of these assignments, the binding interface between this folding intermediate and its protein folding helper enzyme SlyD* could be characterized at residue resolution during the catalysis of prolyl isomerization. Combining abundant chaperone properties with the very specific isomerization function makes SlyD* a very efficient protein folding helper enzyme. The described NMR approach to combine kinetic information with high structural resolution dis closes new possibilities to investigate Michaelis−Menten complexes and kinetics and more generally enzyme mechanisms.

AUTHOR INFORMATION

Corresponding Author

jochen.balbach@physik.uni halle.de

Present Addresses

[#]Department of Biophysical Chemistry, Lund University, SE 22100 Lund, Sweden.

ACKNOWLEDGMENT

Expression vectors for SlyD* were kindly provided by Chris tian Scholz, Roche Diagnostics, Penzberg, Germany. This work was supported by grants of the DFG (GRK 1026 and SFB 610) and BMBF (ProNet T3). Significant investments into our NMR infrastructure from the European Regional Development Fund (ERDF) by the European Union are also gratefully acknowledged.

REFERENCES

(1) Dobson, C. M. *Trends Biochem. Sci.* **1999**, *24*, 329.

(2) Kelly, S. M.; Price, N. C. *Curr. Protoc. Protein Sci.* **2006**, *Charper 20*, No. Unit 20.10.

(3) Royer, C. A. *Chem. Rev* **2006**, *106*, 1769.
(4) Schuler, B.; Eaton, W. A. *Curr. Opin. Struct. Biol.* **2008**, *18*, 16.
(5) Balbach, J.; Steegborn, C.; Schindler, T.; Schmid, F. X. *J. Mol. Biol.* **1999**, *285*, 829.
(6) Dyson, H. J.; Wright, P. E. *Nat. Rev. Mol. Cell Biol.* **2005**, *6*, 197.
(7) Korzhnev, D. M.; Kay, L. E. *Acc. Chem. Res.* **2008**, *41*, 442.
(8) Bartlett, A.; Radford, S. E. *Nat. Struct. Mol. Biol.* **2009**, *16*, 582.
(9) Fersht, A. R. *Proc. Natl. Acad. Sci. U.S.A.* **2000**, *97*, 1525.
(10) Jackson, S. E. *Folding Des.* **1998**, *3*, R81.
(11) Schindler, T.; Herrler, M.; Marahiel, M. A.; Schmid, F. X. *Nat. Struct. Biol.* **1995**, *2*, 663.
(12) Eaton, W. A.; Munoz, V.; Hagen, S. J.; Jas, G. S.; Lapidus, L. J.; Henry, E. R.; Hofrichter, J. *Annu. Rev. Biophys. Biomol. Struct.* **2000**, *29*, 327.
(13) Ferguson, N.; Fersht, A. R. *Curr. Opin. Struct. Biol.* **2003**, *13*, 75.
(14) Jahn, T. R.; Radford, S. E. *FEBS J.* **2005**, *272*, 5962.
(15) Dobson, C. M. *Nature* **2003**, *426*, 884.
(16) Dobson, C. M. *Semin. Cell Dev. Biol.* **2004**, *15*, 3.
(17) Bukau, B.; Deuerling, E.; Pfund, C.; Craig, E. A. *Cell* **2000**, *101*, 119.
(18) Young, J. C.; Agashe, V. R.; Siegers, K.; Hartl, F. U. *Nat. Rev. Mol. Cell Biol.* **2004**, *5*, 781.
(19) Walter, S.; Buchner, J. *Angew. Chem., Int. Ed.* **2002**, *41*, 1098.
(20) Collet, J. F.; Riemer, J.; Bader, M. W.; Bardwell, J. C. *J. Biol. Chem.* **2002**, *277*, 26886.
(21) Fischer, G.; Wittmann Liebold, B.; Lang, K.; Kiefhaber, T.; Schmid, F. X. *Nature* **1989**, *337*, 476.
(22) Rouviere, P. E.; Gross, C. A. *Gene Dev.* **1996**, *10*, 3170.
(23) Ramm, K.; Plückthun, A. *J. Biol. Chem.* **2000**, *275*, 17106.
(24) Ramm, K.; Plückthun, A. *J. Mol. Biol.* **2001**, *310*, 485.
(25) Saul, F. A.; Arie, J. P.; Vulliez le Normand, B.; Kahn, R.; Betton, J. M.; Bentley, G. A. *J. Mol. Biol.* **2004**, *335*, 595.
(26) Scholz, C.; Stoller, G.; Zarnt, T.; Fischer, G.; Schmid, F. X. *EMBO J.* **1997**, *16*, 54.
(27) Hesterkamp, T.; Bukau, B. *FEBS Lett.* **1996**, *389*, 32.
(28) Stoller, G.; Rücknagel, K. P.; Nierhaus, K.; Schmid, F. X.; Fischer, G.; Rahfeld, J. U. *EMBO J.* **1995**, *14*, 4939.
(29) Suzuki, R.; Nagata, K.; Yumoto, F.; Kawakami, M.; Nemoto, N.; Furutani, M.; Adachi, K.; Maruyama, T.; Tanokura, M. *J. Mol. Biol.* **2003**, *328*, 1149.
(30) Wülfing, C.; Lombardero, J.; Plückthun, A. *J. Biol. Chem.* **1994**, *269*, 2895.
(31) Roof, W. D.; Horne, S. M.; Young, K. D.; Young, R. *J. Biol. Chem.* **1994**, *269*, 2902.
(32) Roof, W. D.; Fang, H. Q.; Young, K. D.; Sun, J.; Young, R. *Mol. Microbiol.* **1997**, *25*, 1031.
(33) Scholz, C.; Eckert, B.; Hagn, F.; Schaarschmidt, P.; Balbach, J.; Schmid, F. X. *Biochemistry* **2006**, *45*, 20.
(34) Scholz, C.; Schaarschmidt, P.; Engel, A. M.; Andres, H.; Schmitt, U.; Faatz, E.; Balbach, J.; Schmid, F. X. *J. Mol. Biol.* **2005**, *345*, 1229.
(35) Weininger, U.; Haupt, C.; Schweimer, K.; Graubner, W.; Kovermann, M.; Brüser, T.; Scholz, C.; Schaarschmidt, P.; Zoldak, G.; Schmid, F. X.; Balbach, J. *J. Mol. Biol.* **2009**, *387*, 295.
(36) Martino, L.; He, Y.; Hands Taylor, K. L.; Valentine, E. R.; Kelly, G.; Giancola, C.; Conte, M. R. *FEBS J.* **2009**, *276*, 4529.
(37) Hottenrott, S.; Schumann, T.; Plückthun, A.; Fischer, G.; Rahfeld, J. U. *J. Biol. Chem.* **1997**, *272*, 15697.
(38) Löw, C.; Neumann, P.; Tidow, H.; Weininger, U.; Haupt, C.; Friedrich Epler, B.; Scholz, C.; Stubbs, M. T.; Balbach, J. *J. Mol. Biol.* **2010**, *398*, 375.
(39) Zhang, J. W.; Butland, G.; Greenblatt, J. F.; Emili, A.; Zamble, D. B. *J. Biol. Chem.* **2005**, *280*, 4360.
(40) Zhang, J. W.; Leach, M. R.; Zamble, D. B. *J. Bacteriol.* **2007**, *189*, 7942.
(41) Leach, M. R.; Zhang, J. W.; Zamble, D. B. *J. Biol. Chem.* **2007**, *282*, 16177.
(42) Graubner, W.; Schierhorn, A.; Brüser, T. *J. Biol. Chem.* **2007**, *282*, 7116.
(43) Kiefhaber, T.; Grunert, H. P.; Hahn, U.; Schmid, F. X. *Bio chemistry* **1990**, *29*, 6475.
(44) Kiefhaber, T.; Quaas, R.; Hahn, U.; Schmid, F. X. *Biochemistry* **1990**, *29*, 3061.
(45) Kiefhaber, T.; Quaas, R.; Hahn, U.; Schmid, F. X. *Biochemistry* **1990**, *29*, 3053.
(46) Kiefhaber, T.; Schmid, F. X.; Willaert, K.; Engelborghs, Y.; Chaffotte, A. *Protein Sci.* **1992**, *1*, 1162.
(47) Heinemann, U.; Hahn, U. Structural and functional studies of ribonuclease T1. In *Protein Nucleic Acid Interaction*; Saenger, W.; Heinemann, U., Eds.; MacMillan: London, 1989; p 111.
(48) Mücke, M.; Schmid, F. X. *Biochemistry* **1994**, *33*, 14608.
(49) Steegborn, C.; Schneider Hassloff, H.; Zeeb, M.; Balbach, J. *Biochemistry* **2000**, *39*, 7910.
(50) Balbach, J.; Forge, V.; van Nuland, N. A. J.; Winder, S. L.; Hore, P. J.; Dobson, C. M. *Nat. Struct. Biol.* **1995**, *2*, 865.
(51) Schlepckow, K.; Wirmer, J.; Bachmann, A.; Kiefhaber, T.; Schwalbe, H. *J. Mol. Biol.* **2008**, *378*, 686.
(52) Hore, P. J.; Winder, S. L.; Roberts, C. H.; Dobson, C. M. *J. Am. Chem. Soc.* **1997**, *119*, 5049.
(53) Mok, K. H.; Hore, P. J. *Methods* **2004**, *34*, 75.
(54) Bhuyan, A. K.; Udgaonkar, J. B. *Biochemistry* **1999**, *38*, 9158.
(55) Killick, T. R.; Freund, S. M.; Fersht, A. R. *Protein Sci.* **1999**, *8*, 1286.
(56) Balbach, J.; Forge, V.; Lau, W. S.; van Nuland, N. A. J.; Brew, K.; Dobson, C. M. *Science* **1996**, *274*, 1161.
(57) Felli, I. C.; Brutscher, B. *Chem. Phys. Chem.* **2009**, *10*, 1356.
(58) Szyperski, T.; Atreya, H. S. *Magn. Reson. Chem.* **2006**, *44*, S51.
(59) Freeman, R.; Kupce, E. *Concepts Magn. Reson., Part A* **2004**, *23A*, 63.
(60) Szyperski, T.; Wider, G.; Bushweller, J. H.; Wuthrich, K. *J. Biomol. NMR* **1993**, *3*, 127.
(61) Kupce, E.; Freeman, R. *J. Am. Chem. Soc.* **2004**, *126*, 6429.
(62) Kupce, E.; Freeman, R. *J. Biomol. NMR* **2003**, *25*, 349.
(63) Brutscher *J. Biomol. NMR* **2004**, *29*, 57.
(64) Frydman, L.; Scherf, T.; Lupulescu, A. *Proc. Natl. Acad. Sci. U.S.A.* **2002**, *99*, 15858.
(65) Hyberts, S. G.; Takeuchi, K.; Wagner, G. *J. Am. Chem. Soc.* **2010**, *132*, 2145.
(66) Ernst, R. R.; Bodenhausen, G.; Wokaun, A. *Principles of Nuclear Magnetic Resonance in One and Two Dimensions*; Oxford University Press: Oxford, 1987; p 124.
(67) Ross, A.; Salzman, M.; Senn, H. *J. Biomol. NMR* **1997**, *10*, 389.
(68) Lescop, E.; Schanda, P.; Brutscher, B. *J. Magn. Reson.* **2007**, *187*, 163.
(69) Pervushin, K.; Vögeli, B.; Eletsky, A. *J. Am. Chem. Soc.* **2002**, *124*, 12898.
(70) Schanda, P.; Brutscher, B. *J. Am. Chem. Soc.* **2005**, *127*, 8014.
(71) Schanda, P.; Forge, V.; Brutscher, B. *Proc. Natl. Acad. Sci. U.S.A.* **2007**, *104*, 11257.
(72) Schanda, P.; Kupce, E.; Brutscher, B. *J. Biomol. NMR* **2005**, *33*, 199.
(73) Schanda, P.; Van Melckebeke, H.; Brutscher, B. *J. Am. Chem. Soc.* **2006**, *128*, 9042.
(74) Corazza, A.; Rennella, E.; Schanda, P.; Mimmi, M. C.; Cutuil, T.; Raimondi, S.; Giorgetti, S.; Fogolari, F.; Viglino, P.; Frydman, L.; Gal, M.; Bellotti, V.; Brutscher, B.; Esposito, G. *J. Biol. Chem.* **2010**, *285*, 5827.
(75) Mücke, M.; Schmid, F. X. *J. Mol. Biol.* **1994**, *239*, 713.
(76) Löw, C.; Neumann, P.; Tidow, H.; Weininger, U.; Haupt, C.; Friedrich Epler, B.; Scholz, C.; Stubbs, M. T.; Balbach, J. *J. Mol. Biol.* **2010**, *398*, 375 390.
(77) Haupt, C.; Weininger, U.; Kovermann, M.; Balbach, J. *Biochem istry* **2011**, submitted for publication.
(78) Delaglio, F.; Grzesiek, S.; Vuister, G. W.; Zhu, G.; Pfeifer, J.; Bax, A. *J. Biomol. NMR* **1995**, *6*, 277.
(79) Johnson, B. A. *Methods Mol. Biol.* **2004**, *278*, 313.
(80) Weininger, U.; Jakob, R. P.; Eckert, B.; Schweimer, K.; Schmid, F. X.; Balbach, J. *Proc. Natl. Acad. Sci. U.S.A.* **2009**, *106*, 12335.

(81) Neal, S.; Nip, A. M.; Zhang, H.; Wishart, D. S. *J. Biomol. NMR* **2003**, *26*, 215 240.
(82) Zeeb, M.; Balbach, J. *Methods* **2004**, *34*, 65.
(83) Aumüller, T.; Fischer, G. *J. Mol. Biol.* **2008**, *376*, 1478.
(84) Knappe, T. A.; Eckert, B.; Schaarschmidt, P.; Scholz, C.; Schmid, F. X. *J. Mol. Biol.* **2007**, *368*, 1458.
(85) Scholz, C.; Thirault, L.; Schaarschmidt, P.; Zarnt, T.; Faatz, E.; Engel, A. M.; Upmeier, B.; Bollhagen, R.; Eckert, B.; Schmid, F. X. *Biochemistry* **2008**, *47*, 4276.
(86) Benanti, E. L.; Chivers, P. T. *J. Bacteriol.* **2009**, *191*, 2405.
(87) Stingl, K.; Schauer, K.; Ecobichon, C.; Labigne, A.; Lenormand, P.; Rousselle, J. C.; Namane, A.; de Reuse, H. *Mol. Cell Proteomics* **2008**, *7*, 2429.
(88) Han, K. Y.; Song, J. A.; Ahn, K. Y.; Park, J. S.; Seo, H. S.; Lee, J. *Protein Eng. Des. Sel.* **2007**, *20*, 543.